NASA Shell Buckling Knockdown Factor Project

Dr. Mark W. Hilburger
Dr. Marc R. Schultz

May 2022

Outline

- Background
- Problem Description
- Project Objectives and Approach
- Project Overview and Achievements
- Highlighted Results
- Concluding Remarks

Launch-Vehicle Shell Structures

- **Cylindrical shells**
  - **Significant portion of launch-vehicle structure**
- **Buckling**
  - **Often a controlling failure mode during design**
  - **Empirical buckling loads are often significantly less than theoretical predictions**

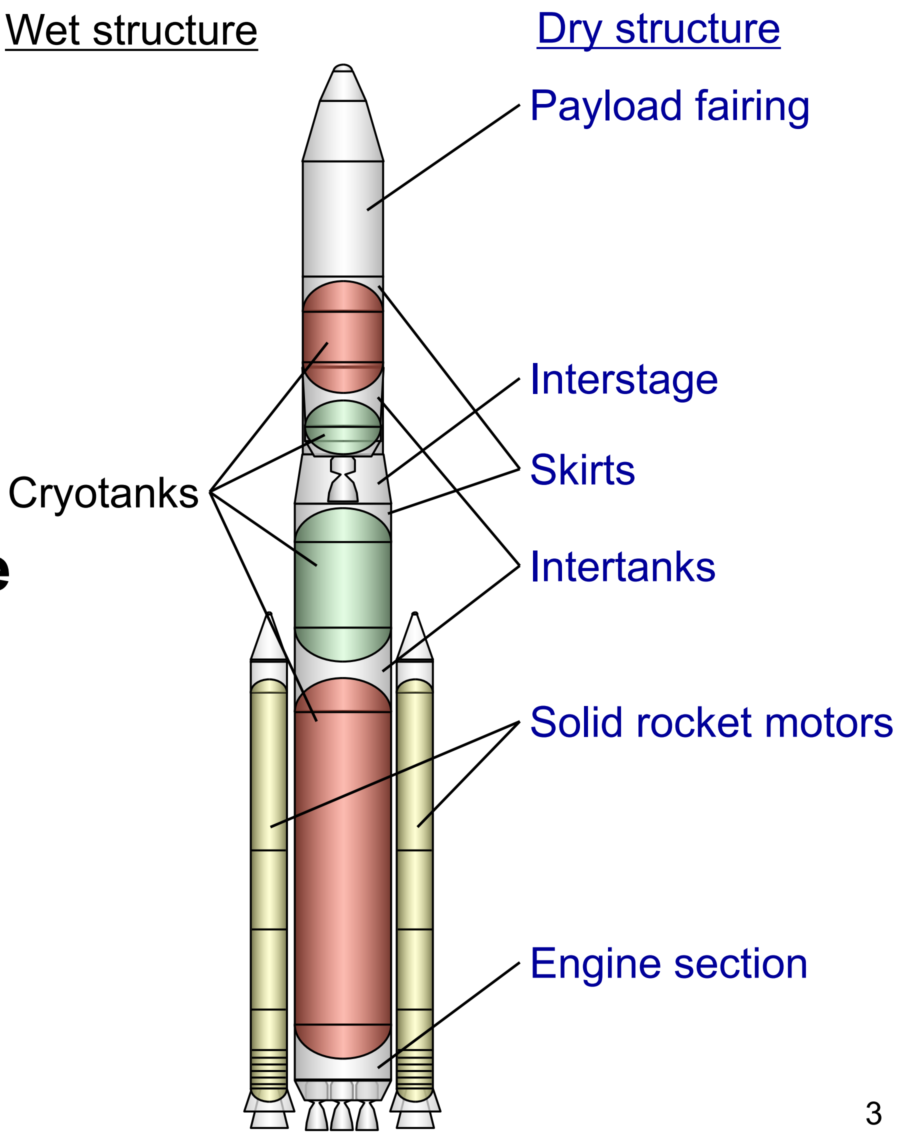

Empirical Shell-Buckling Design Approach

- **Standard practice is to predict the buckling load of an idealized perfect cylinder and apply an empirical *buckling knockdown factor (KDF)* to account for differences between test and analysis**
- **Differences between test and analysis primarily attributed to initial *geometric imperfections* in the shell wall (i.e., out-of-roundness)**

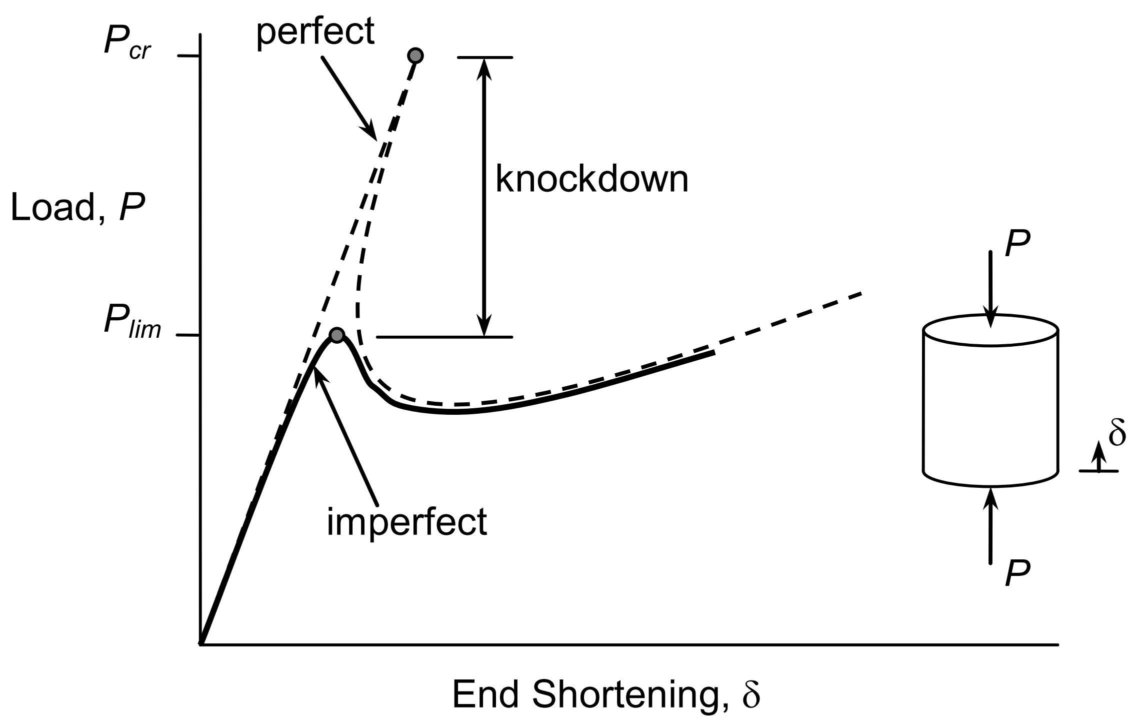

Typical Knockdown Factors

Buckling of Thin-Walled Cylinders, NASA SP-8007, 1968

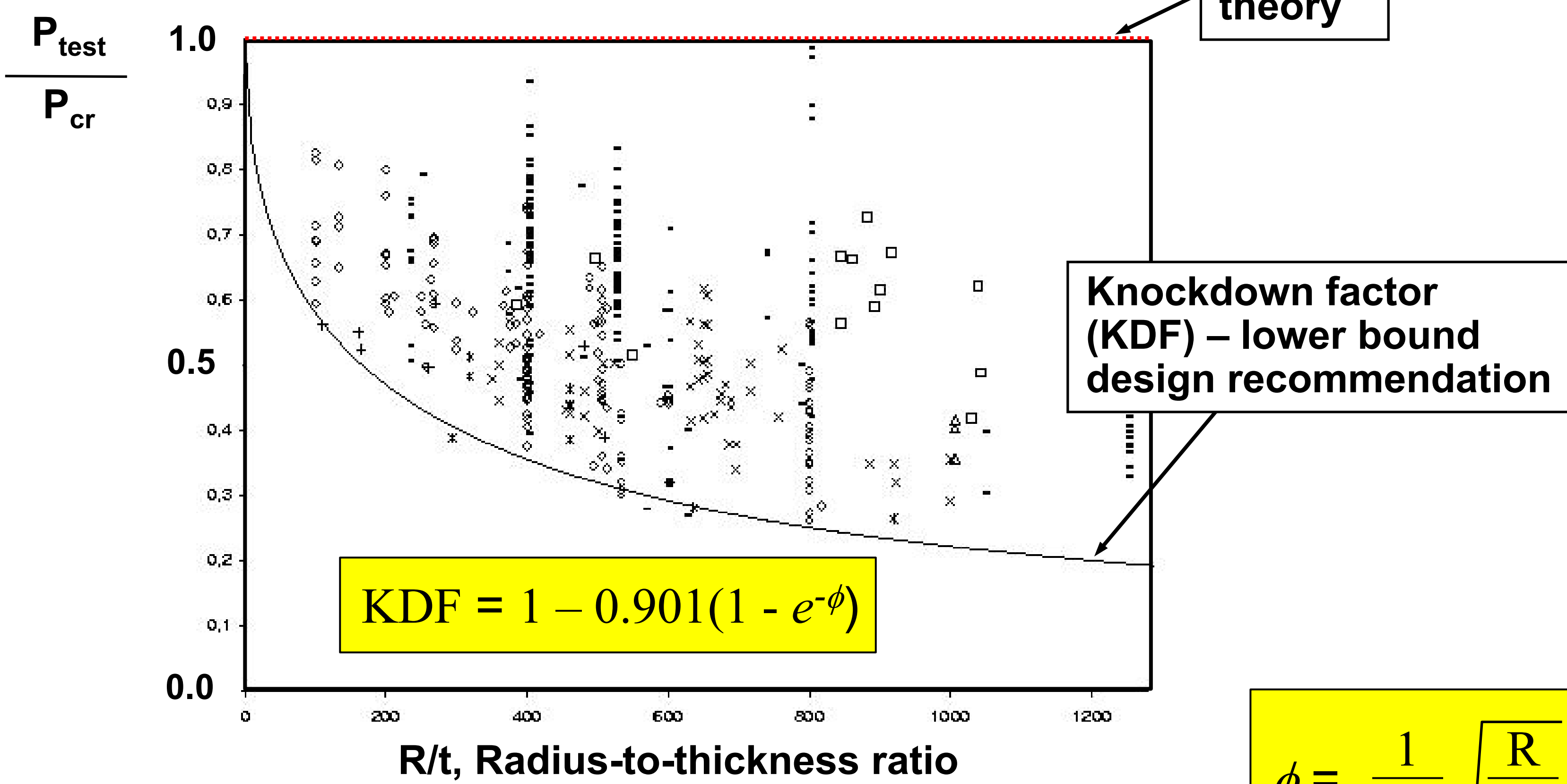

$$\text{KDF} = 1 - 0.901(1 - e^{-\phi})$$

$$\phi = \frac{1}{16}\sqrt{\frac{R}{t}}$$

Deficiencies of Historic Knockdown Factors

- The recommended KDFs for use in the design of aerospace-quality shell structures are typically overly conservative as indicated by test results
  - Conservative → large weight penalty
    - Example: Space Shuttle LH_2 tank designed to 140%LL, tested to > 200%LL
- Pedigree of the test data used to develop the design KDFs is often difficult to assess, and in some cases undocumented and thus critical reviews of the existing data are limited
  - Effects of geometric imperfections not well understood until 1950s
  - Boundary conditions assumed to be a secondary effect
  - Large scatter in test data
- Design information is not available for shells constructed from modern materials and manufacturing processes (e.g., composite shells or friction-stir-welded aluminum (Al) alloy shells)
  - Limited data for stiffened cylinders
  - No data for composite cylinders
- The design recommendations and data do not provide information necessary to quantify robustness and reliability

Problem Description

- Buckling is often the critical consideration in the design of thin-walled aerospace shell structures
  - Reliable, validated design criteria are needed for shells fabricated with advanced materials and manufacturing techniques

- The primary limitations in the existing design practice, included the following:
  - Knockdown factors used in the design of aerospace-quality shell structures were typically overly conservative
  - The pedigree of the test data used to develop the design knockdown factors was often difficult to assess, and in some cases undocumented
  - Design information was not available for shells constructed from modern materials and manufacturing processes such as composite shells or friction-stir-welded aluminum alloy shells
  - The design recommendations and data did not provide information necessary to quantify robustness and reliability

Project Objectives

- To develop and validate new analysis-based shell buckling knockdown factors (KDF) and design guidelines for launch-vehicle structures
  - Metallic cryotank and dry structures
  - Composite dry structures

- Provide updated NASA SP-8007

- Implement new KDFs in the development of NASA's new heavy-lift launch vehicle

Project Approach

- **Design trade studies**
  - Identify candidate high-payoff launch vehicle structural configurations for the development of analysis-based knockdown factors and structural testing
- **Develop and assess various analysis-based knockdown factor prediction methodologies**
- **Targeted validation testing at coupon, panel, and cylinder levels with detailed test and analysis correlation**
  - Relevant subscale and full-scale test-article designs that span the launch-vehicle design space
  - State-of-the-art manufacturing, testing, and measurement techniques
- **Develop shell buckling knockdown factors and analysis methods for relevant launch vehicle structural configurations**
  - Multicenter, multiorganization team
  - Engage the user community through workshops
  - Domestic and International collaborations

Summary of SBKF Testing and Analysis Efforts

- **Large-scale testing/test analysis correlation**
  - 8-ft-diameter metallic cylinders
  - 27.5-ft-diameter metallic cylinders
  - 8-ft-diameter composite cylinders

- **Coupon, panel, and subcomponent testing**
  - Metallic
    - Aluminum-Lithium (Al-Li) 2050 testing
    - Stiffener crippling
  - Composite
    - Fluted-core testing

Large-Scale Validation Testing

- 8-ft-diameter and 27.5-ft-diameter test articles
- For validation of analysis methods
- Testing at MSFC
- Test articles designed to representative of launch-vehicle structures
- Highly instrumented
  - Strain gages
  - Displacement sensors
  - Low-speed digital image correlation (DIC)
  - High-speed DIC
  - Microphones
  - High-definition video
- Test-analysis correlation

8-ft-diameter test setup

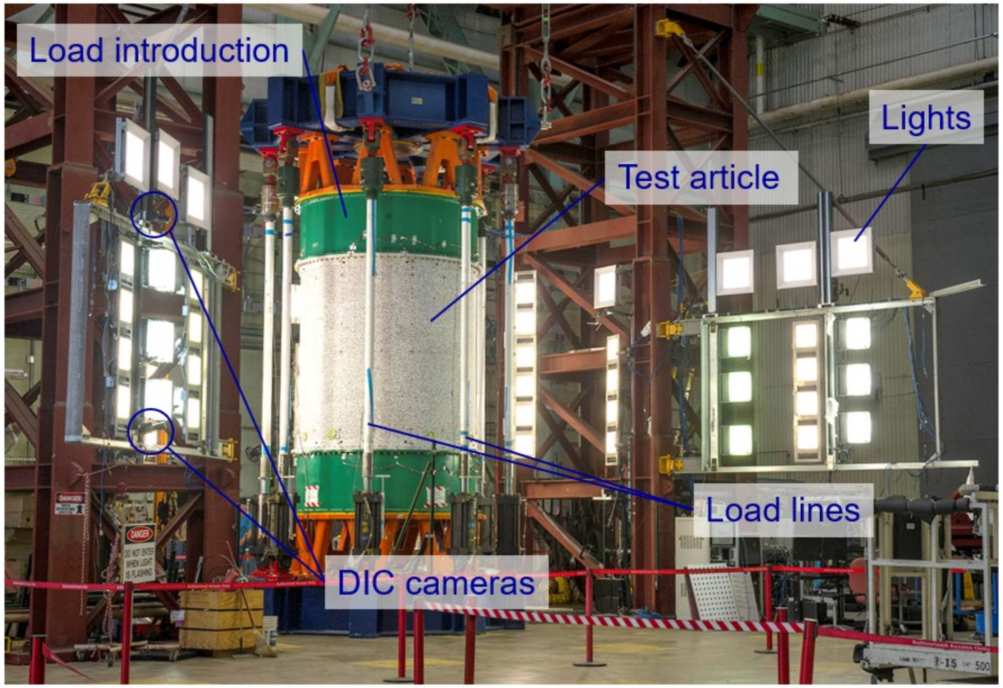

Large-Scale Validation Testing: Metallic

Eight welded integrally stiffened aluminum lithium (AL-Li) alloy 8-ft-diameter cylinders

Fabrication

Machining (AMRO)

Welding (MSFC)

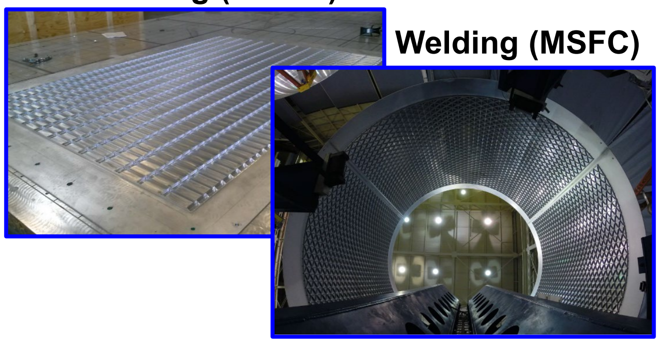

Measured radial imperfections

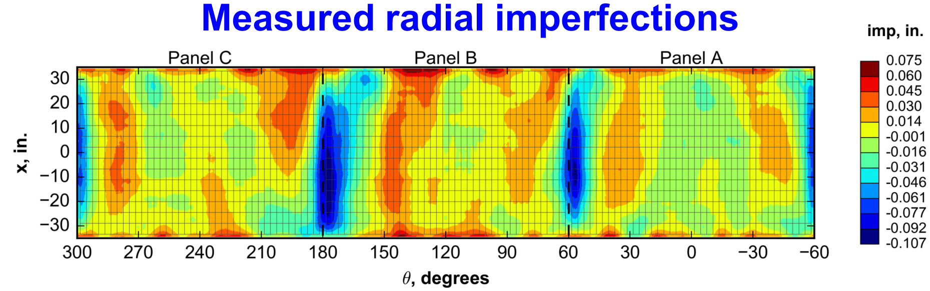

Post-buckled shape

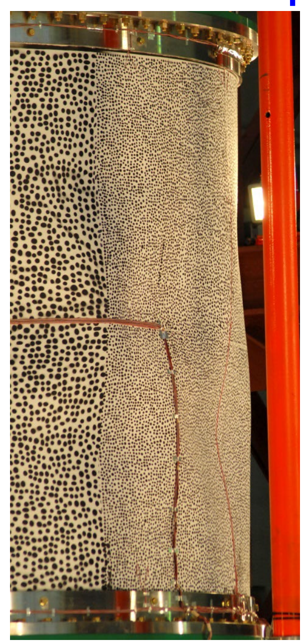

Finite element model

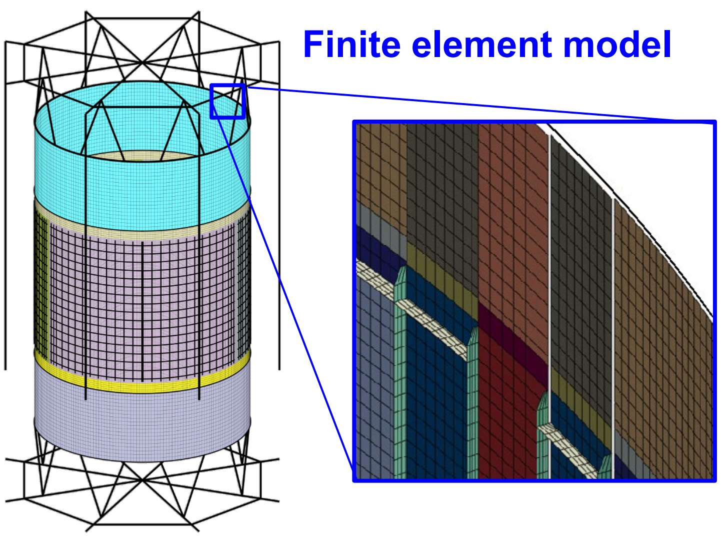

Radial displacements at failure

Pretest prediction

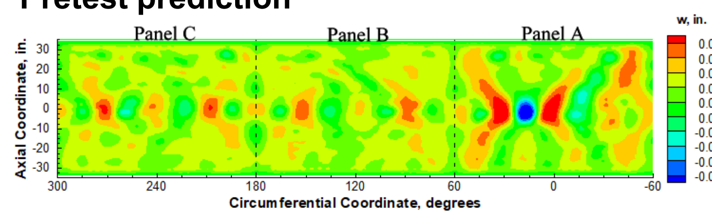

Test (DIC)

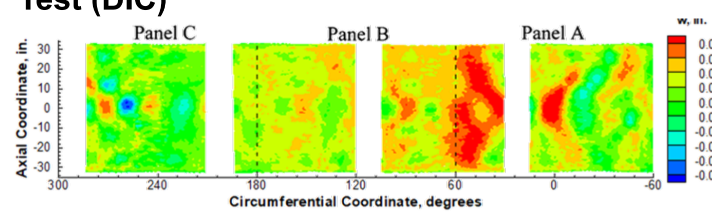

Large-Scale Validation Testing: Metallic

Two 27.5-ft-diameter cylinders from excess Space Shuttle External Tank panels

Welding & Machining (MSFC)

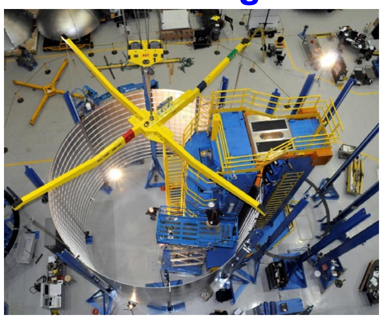

Test-article assembly

Finite element model

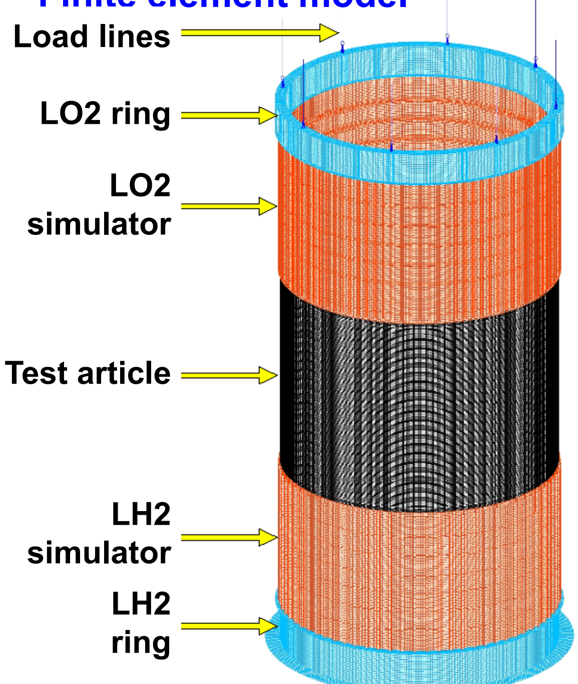

Pocket buckling

Pretest prediction

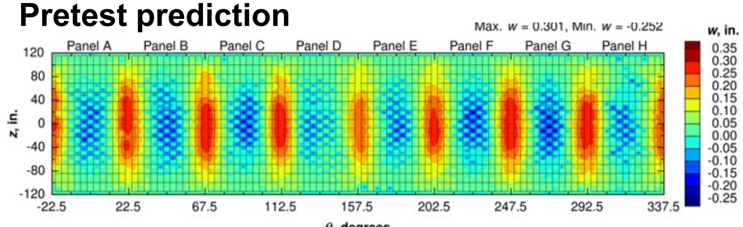

Test (DIC)

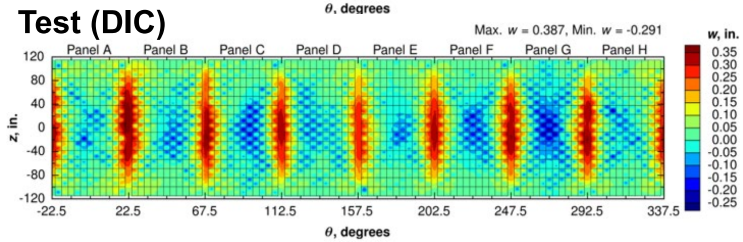

Additional Metallic Work

- **Aluminum lithium (Al-Li) alloy 2050 material property testing**
  - Potential alternate to Al-Li 2195 available in larger plate
- **Al-Li 2195 stiffener crippling study**
  - Test and analysis of stiffened coupon test articles
  - Better understand stiffener separation and low transverse shear strength

»

- **Buckling test of an orthogrid-stiffened seamless cylinder**
  - Flow-formed Al 2219 8-ft-diameter cylinder with integral machined stiffeners
  - Demonstrated improved structural efficiency versus welded test article

Stiffener crippling coupon test

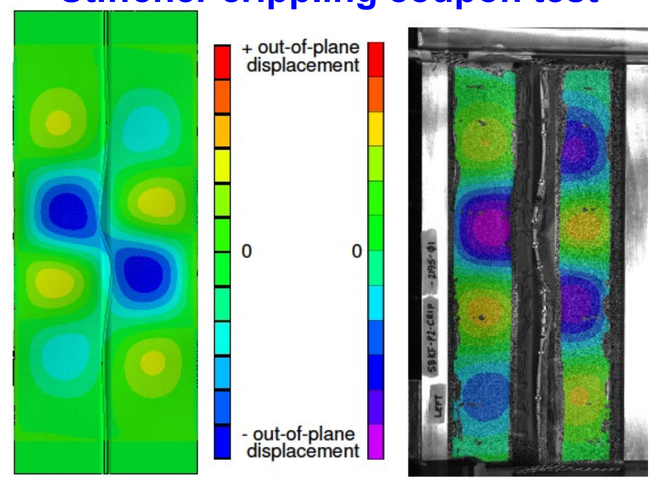

(a) predicted (b) measured, 2195-01

Machining seamless cylinder

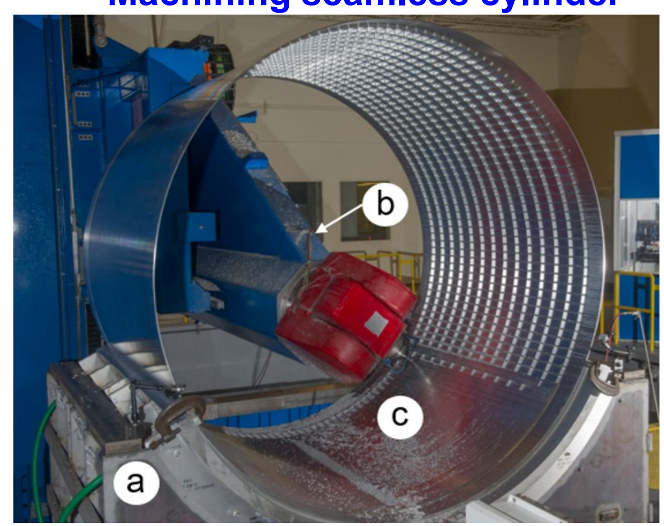

Large-Scale Validation Testing: Composite

Four honeycomb-core sandwich composite 8-ft-diameter cylinders

Fabrication (MSFC)

Radial displacements at failure

Pretest prediction

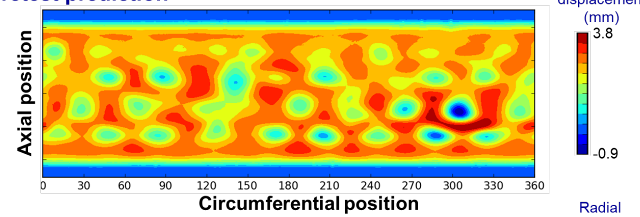

Test (digital image correlation)

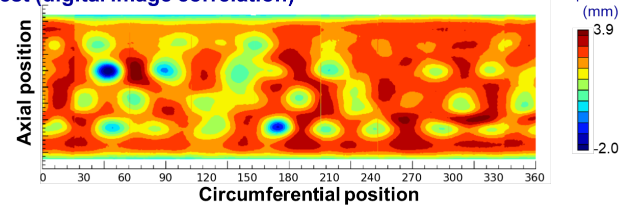

Post failure

Finite element model

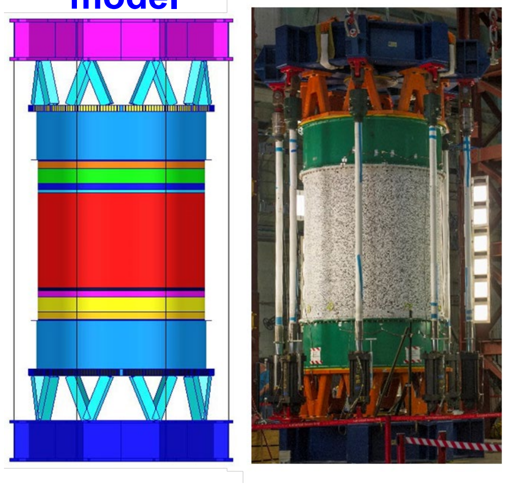

Load-end shortening

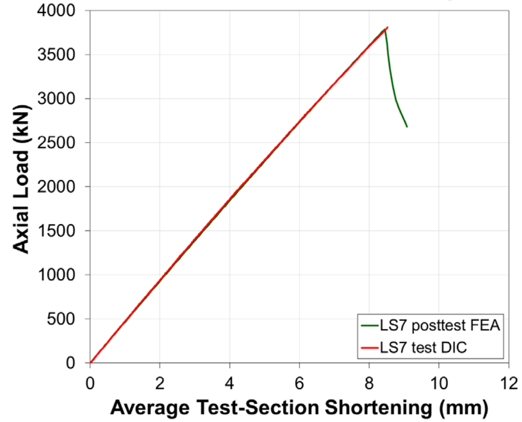

Additional Composite Work

Fluted-Core Sandwich Composite Structures

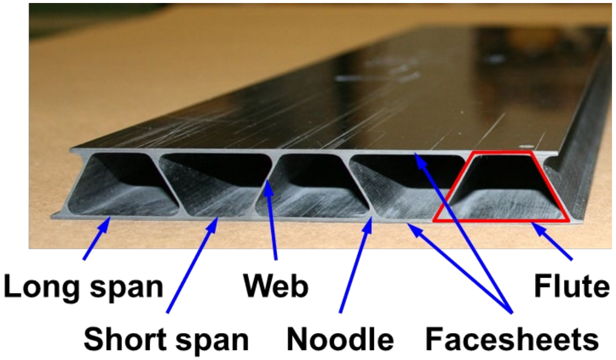

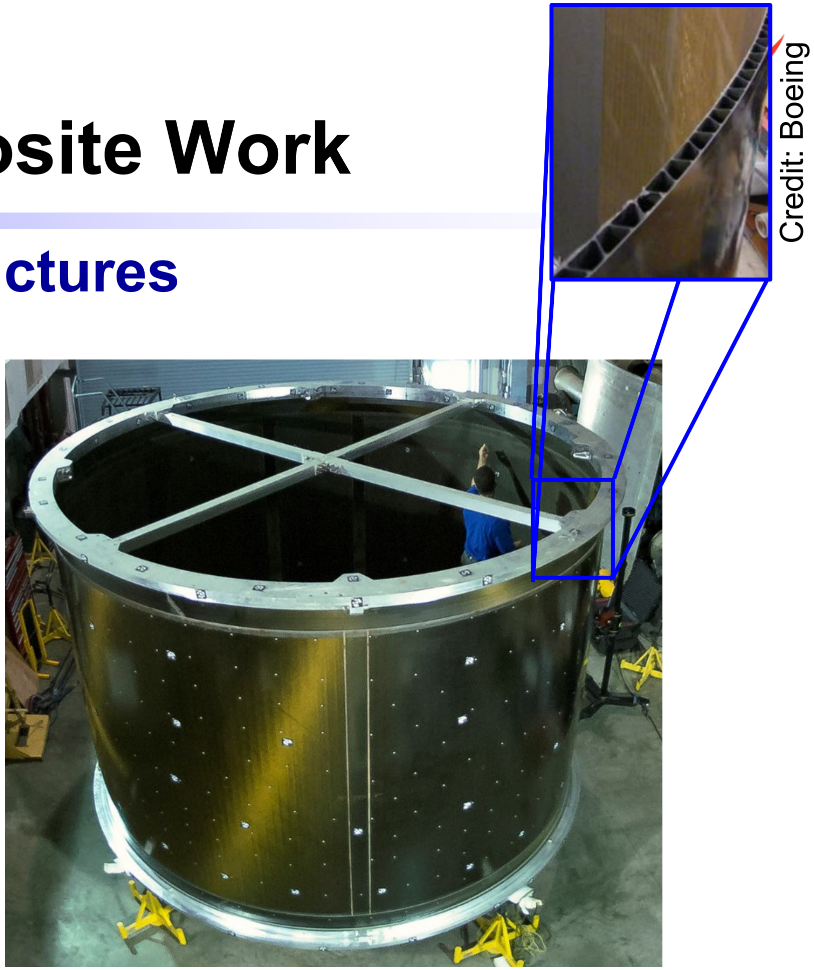

Local buckling
(out-of-plane deformation)

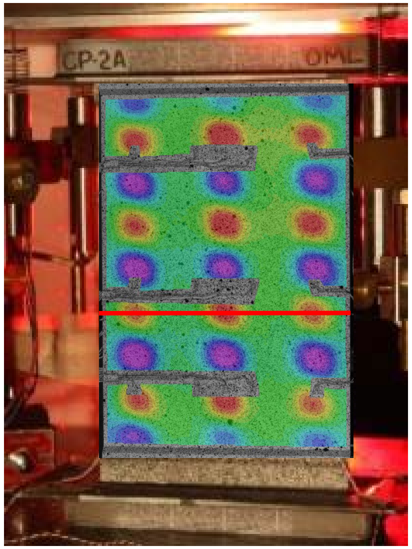

Transverse-shear deformation

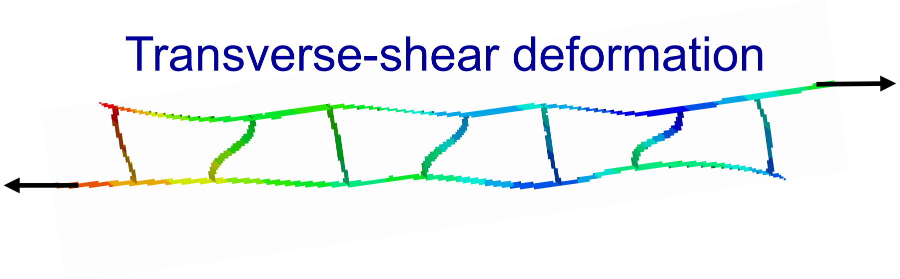

Achievements

- **SLS impacts**
  - KDFs for SLS
    - 2000-3000-lb mass savings in the SLS core stage tanks.
    - Reductions in design and analysis cycle time by eliminating the need for detailed structural optimization of weld lands.
    - Reduced material costs by $300 k to $400 k per vehicle by using thinner plate material (machining cost reduction is also anticipated, but not captured in this estimate).
    - Contributed significantly to on-time Preliminary Design Review (PDR).
    - Future knockdown factors updates could "expand the flight envelope for the core stage and help upgrade the current vehicle to the Block 1b and Block 2 vehicles (supported by margin testing).
  - High-fidelity analysis methods have been used in an independent assessment of the buckling response and design margins of the SLS core stage LH2 (liquid hydrogen) and LOX (liquid oxygen) tanks that were the subject of a PDR RID
  - Provide guidance to SLS in several areas including:
    - interpretation of complex buckling behavior exhibited by the SLS core stage engine structure and instrument
    - test planning and instrumentation recommendations for full-scale structural qualification tests
    - implementation of new analysis-based design approach

Achievements

- **SP-8007 Update**
  - Comprehensive discussion on the State of the Art
    - Identifies important research developments and current trends
    - Establishes the technological basis for the updated criteria and recommended practices
  - Expand the section on Recommended Practices
    - Semi-empirical design approach
    - Analysis-based design approach
  - Advancing the SoA and helping overcome years of empirical design convention

Highlighted Results (General, Metallic)

- **General Buckling**

  G-1. Data collected was used to revise NASA's SP-8007, "Buckling of Thin-Walled Circular Cylinders."
  - Test data to develop and validate a new analysis-based KDF development approach
  - State of the Art assessment that identifies important research developments and current trends and establishes the technological basis for the updated criteria and recommended practices.

- **Metallic Buckling**

  M-1. The design of highly loaded unpressurized structures and tanks with relatively low internal pressures exhibit the large weight savings potential when increasing the KDF (e.g., up to 33.5% weight reduction for Ares-V Interstage).

  M-2. The following details were shown to be important in developing accurate FEM that correlate with large-scale experimental test results of integrally stiffened metallic cylinders:
  - As-manufactured (versus nominal) skin and stiffener thicknesses and stiffener heights,
  - Stiffener fillet (node) representation,
  - Refined representation of compliant boundary conditions, and
  - Inclusion of measured radial imperfections, especially the as-installed imperfection

  M-3. Weld lands can reduce the buckling load of a compression-loaded cylinder.
  - Addition of weld lands to integrally stiffened metallic cylinders led to a predicted reduction in linear buckling load between 1 and 27.6%.

  M-4. Measured geometric imperfections of integrally stiffened cylinders with axial weld lands indicate relatively large magnitude localized imperfections at the weld lands.

Highlighted Result (General)

- **General Buckling**

  G-1. Data collected was used to revise NASA's SP-8007, "Buckling of Thin-Walled Circular Cylinders."

  - **Test data to develop and validate a new analysis-based KDF development approach**
  - **State of the Art assessment that identifies important research developments and current trends and establishes the technological basis for the updated criteria and recommended practices.**

Highlighted Result (Metallic)

- **Metallic Buckling**

  M-1. The design of highly loaded unpressurized structures and tanks with relatively low internal pressures exhibit the large weight savings potential when increasing the KDF (e.g., up to 33.5% weight reduction for Ares-V Interstage).

Ares V
LV_45.0.02_01

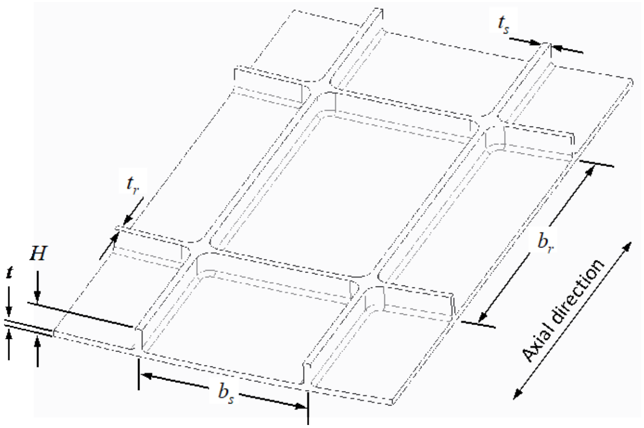

Al-Li
2195
orthogrid

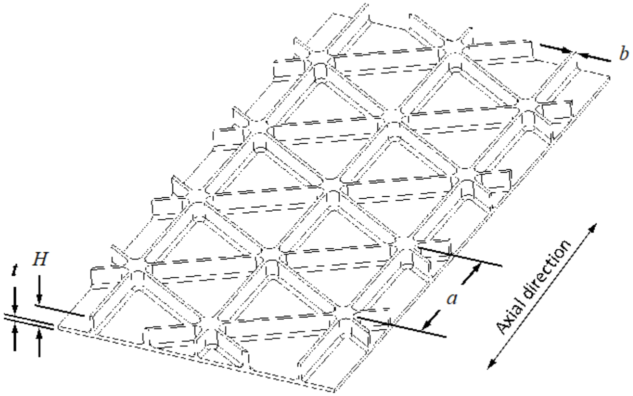

Al-Li
2195
isogrid

Highlighted Result (Metallic), M-1 concluded

- ## Metallic Buckling

  M-1. The design of highly loaded unpressurized structures and tanks with relatively low internal pressures exhibit the large weight savings potential when increasing the KDF (e.g., up to 33.5% weight reduction for Ares-V Interstage).

Design study

Axial load = 3660 lb/in

Internal pressure = 0, 5, 20 psi

γ = 0.65, 0.75, 0.85

$\Delta\gamma$ = 0.14 for internal pressure

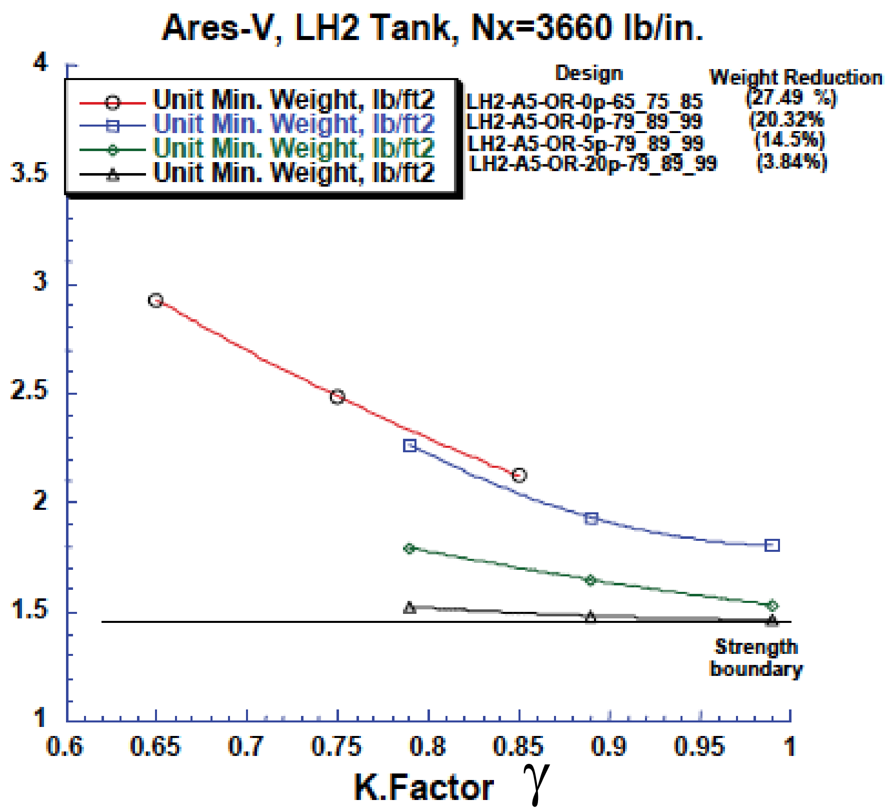

Highlighted Result (Metallic)

- **Metallic Buckling (continued)**

  M-2. The following details were shown to be important in developing accurate FEM that correlate with large-scale experimental test results of integrally stiffened metallic cylinders:
  - **As-manufactured (versus nominal) skin and stiffener thicknesses and stiffener heights,**
  - **Stiffener fillet (node) representation,**
  - **Refined representation of compliant boundary conditions, and**
  - **Inclusion of measured radial imperfections, especially the as-installed imperfection**

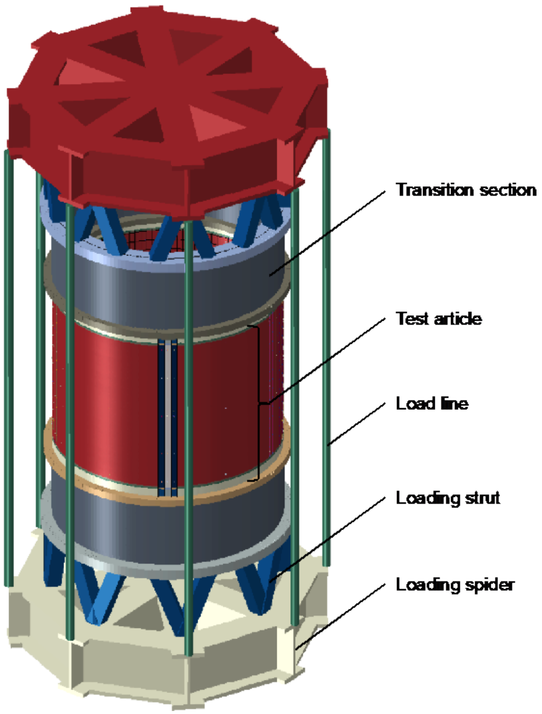

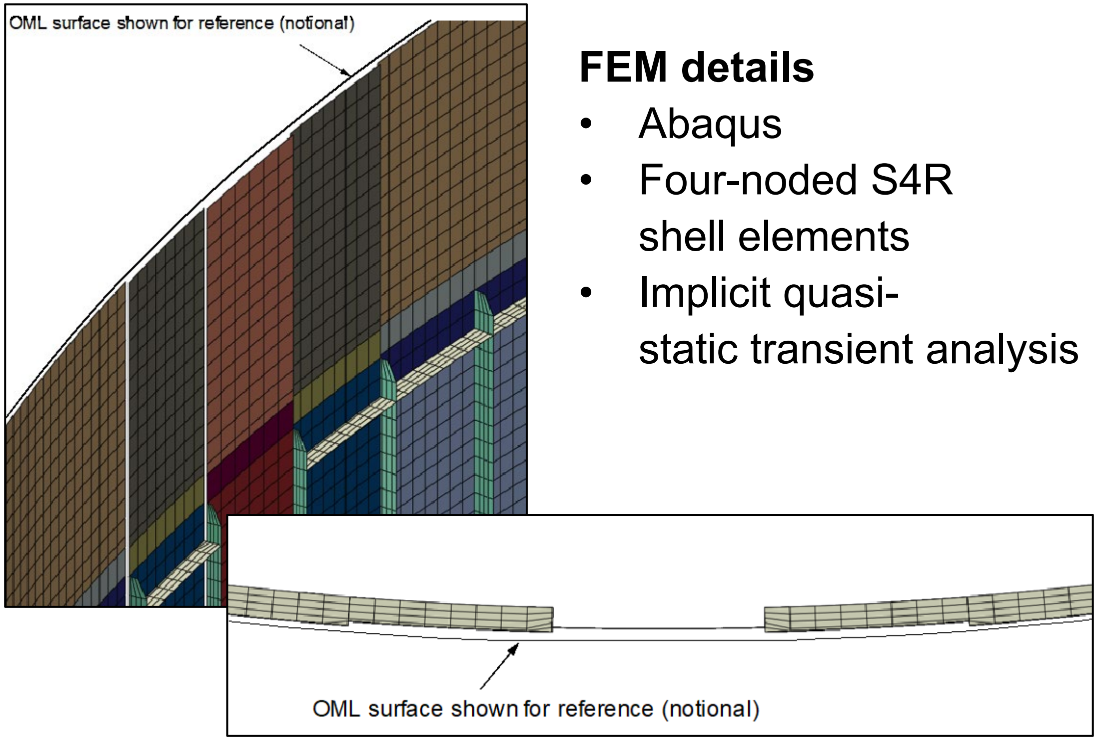

FEM details
- Abaqus
- Four-noded S4R shell elements
- Implicit quasi-static transient analysis

Highlighted Result (Metallic), M-2 continued

Model sensitivity study results for TA07

Model detail	Baseline model assumption	Model adjustment	Change in buckling load	Other
Young's modulus	Uniform modulus, E = 11.0 Msi	Separate compression and tension modulus values, E_c = 11.4 Msi, E_t = 10.8 Msi	1.3%	2.5% increase in effective axial stiffness
Skin and stiffener thicknesses	Nominal, as-designed	Use average measured thicknesses. t = 0.093, t_s = 0.108, t_r = 0.104	7.8%	4.4% increase in effective axial stiffness
Stiffener heights	Nominal, as-designed	Use average measured height, H = 0.445	1.1%	None
Attachment ring model	Steel ring and Al-Li cylinder modeled as a laminate	Model rings as circumferential beams to provide radial constraint and axial compliance	<1.0%	6.3% reduction in effective axial stiffness Change in bending boundary layer response
Attachment ring thru bolt detail	Neglected	Bolt detail modeled using rigid links	1.6%	None
Geometric imperfection	White-light geometry measurement	Measured imperfection amplitude reduced to match DIC-based pretest measurement	4.5%	None
Stiffener fillet representation	Neglected	Local stiffener thicknesses increased based on correlation between 2-D shell model and 3-D solid model	4.2%	None
Attachment ring imperfection	Neglected	Measured attachment ring interface surface geometry measured and included in model	-1.8%	Change in buckling location from weld land A/B to weld land B/C

Highlighted Result (Metallic), M-2 continued

Model sensitivity study results for TA07

Load vs. end-shortening response

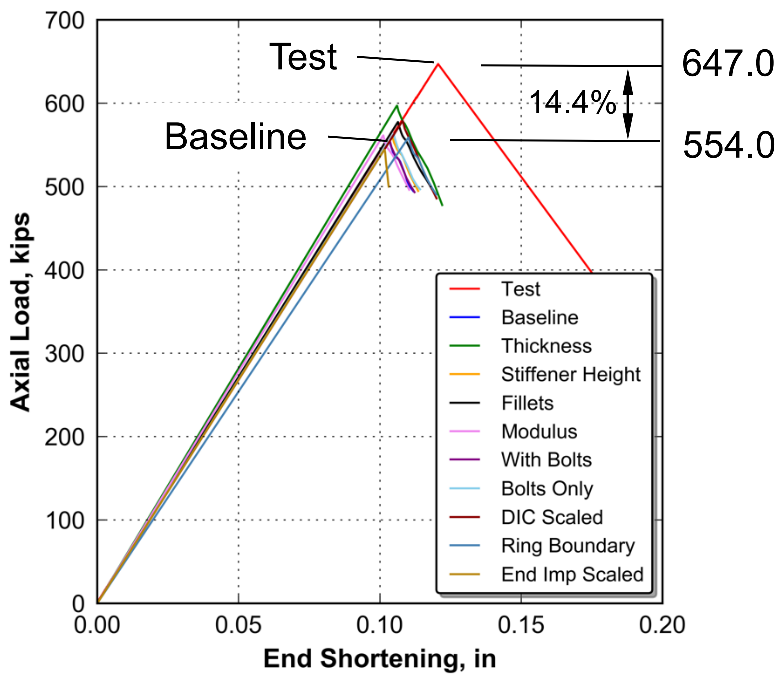

Load vs. weld land radial displacement response

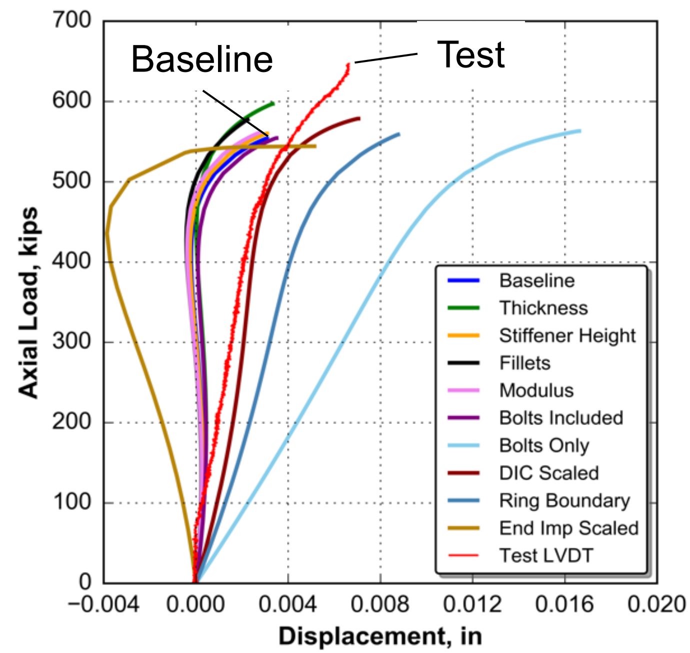

- Some sensitivity in effective axial stiffness and buckling load (left)
- Significant sensitivity in radial displacement response (right)

Highlighted Result (Metallic), M-2 continued

Model sensitivity study results – Improved attachment ring model

Baseline model: Steel ring and Al-Li cylinder modeled as a laminate (stiff)
Improved model: Circumferential rings to provide radial constraint, axially free

a typical test article mesh detail with a modified attachment ring model

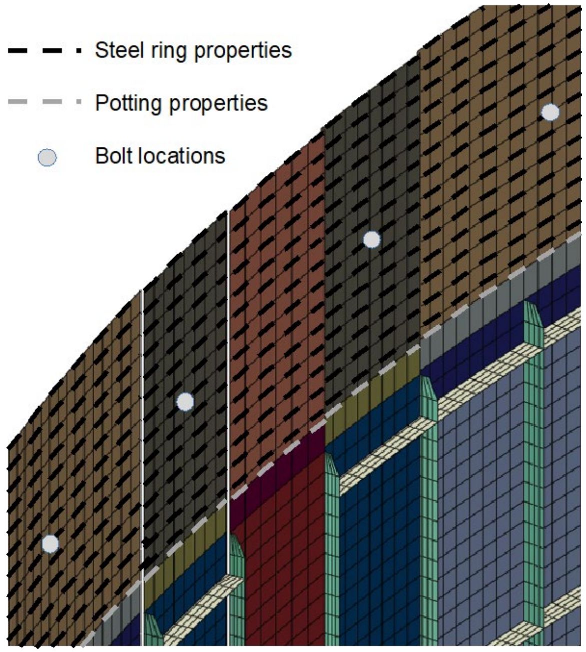

attachment ring cross-section

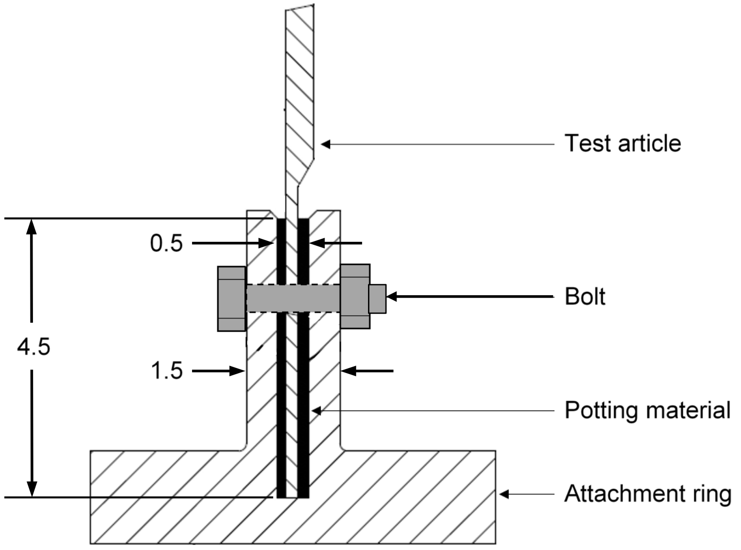

Highlighted Result (Metallic), M-2 continued

Model sensitivity study results – Improved attachment ring model

Measured radial displacement contours

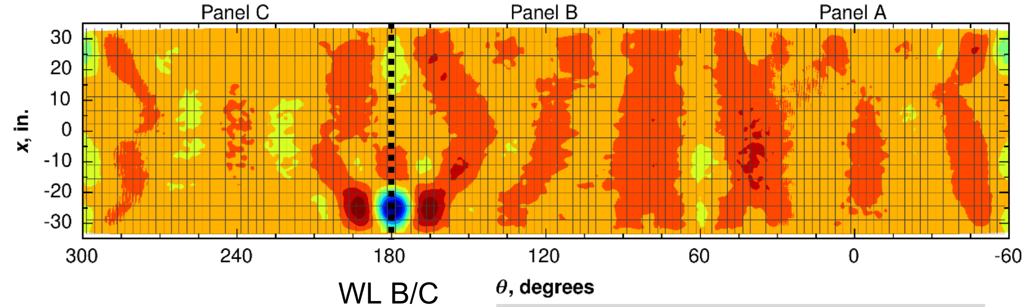

Predicted and measured radial displacement at weld land B/C

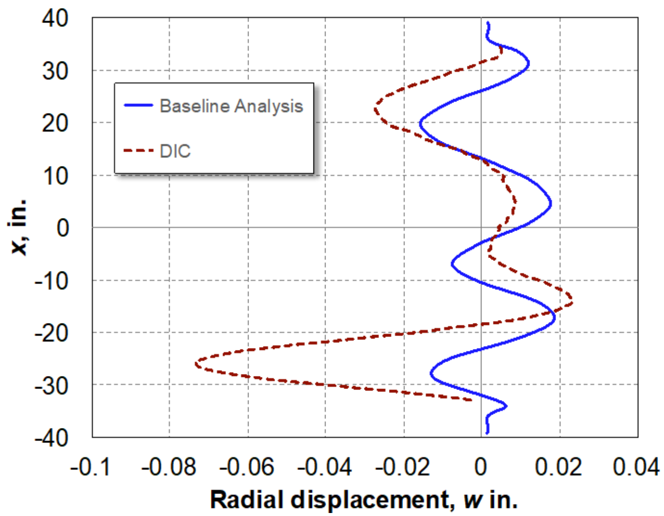

Predicted displacements: Baseline and improved attachment ring model

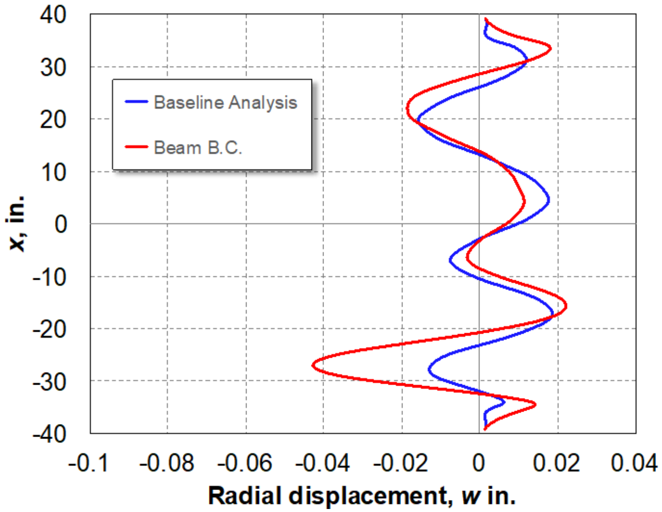

Significant qualitative improvement in predicted displacement response

Highlighted Result (Metallic), M-2 continued

Model sensitivity study results – Stiffener fillet representation

<u>Stiffener fillet representation</u>:
Solid model results were used to "tune" the shell model thicknesses and provide an equivalent shell model representation

Model tuning metrics included
- Axial stiffness
- Local and global buckling response

Shell model

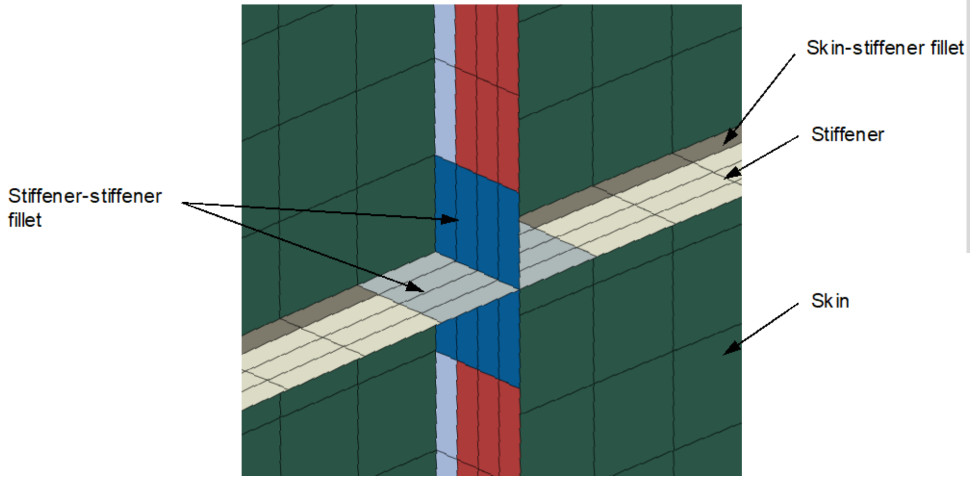

Solid model

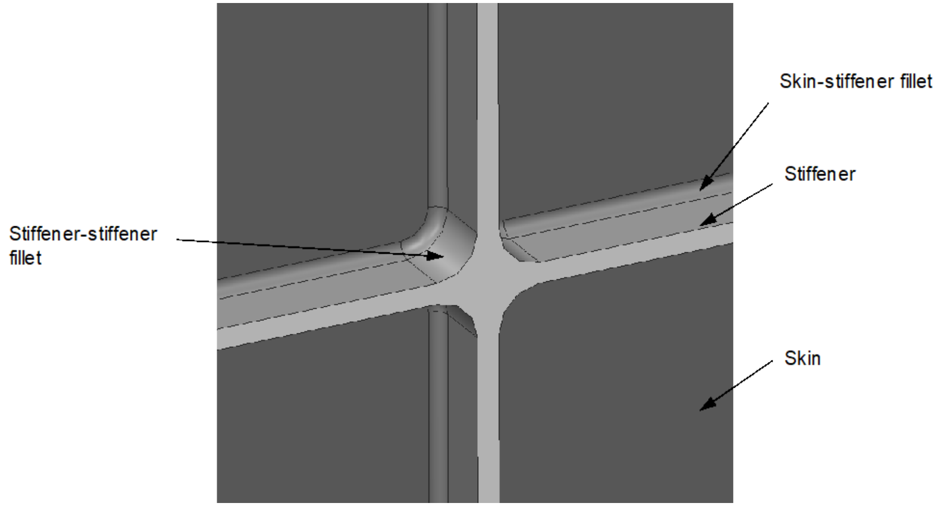

Highlighted Result (Metallic), M-2 continued

Model sensitivity study results – Stiffener fillet representation

Shell model –
Weld land region

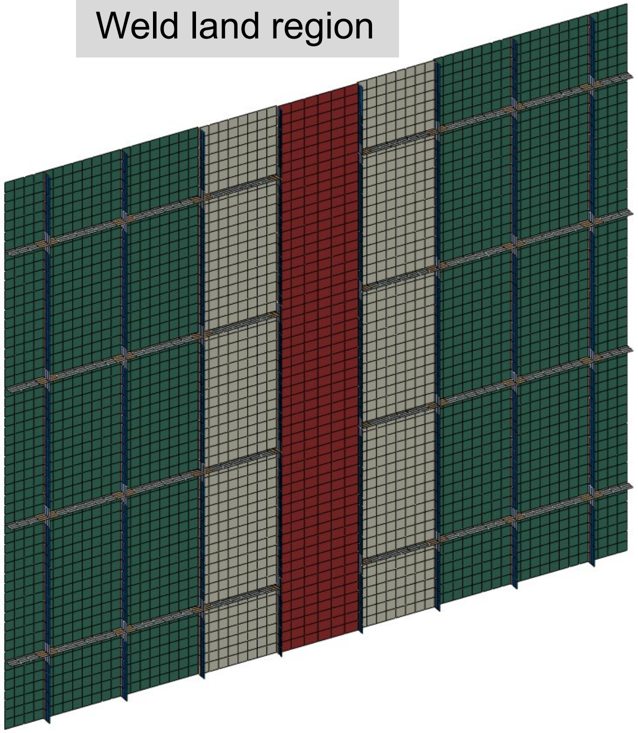

Shell model –
Selected buckling
modes and % error

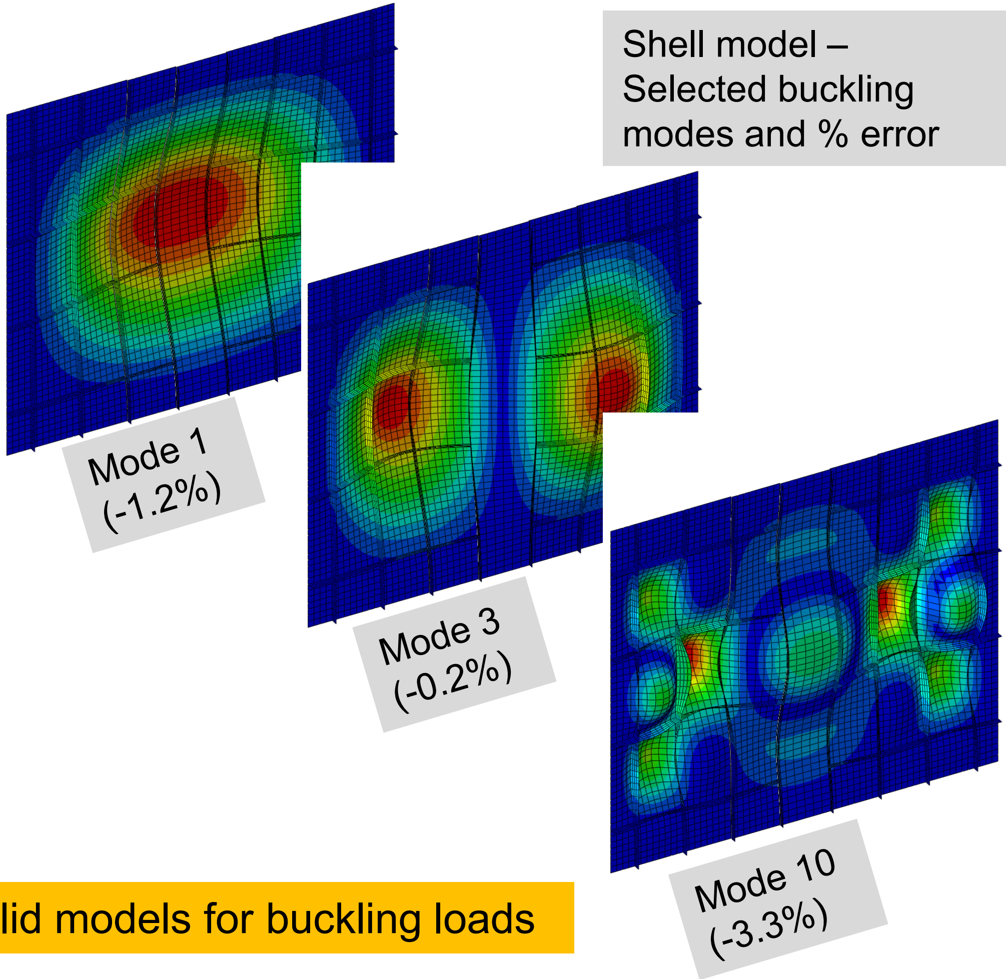

Tuned shell models within ~3% of solid models for buckling loads

Highlighted Result (Metallic), M-2 concluded

Model sensitivity study results – Attachment (End) Imperfection

Attachment ring imperfection measurements

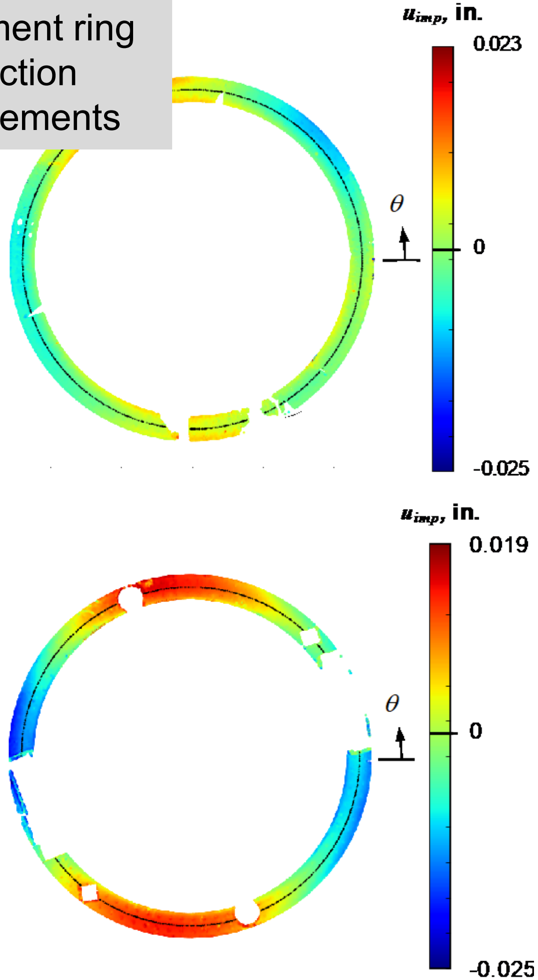

Attachment ring imperfection measurements (circumferential traces)

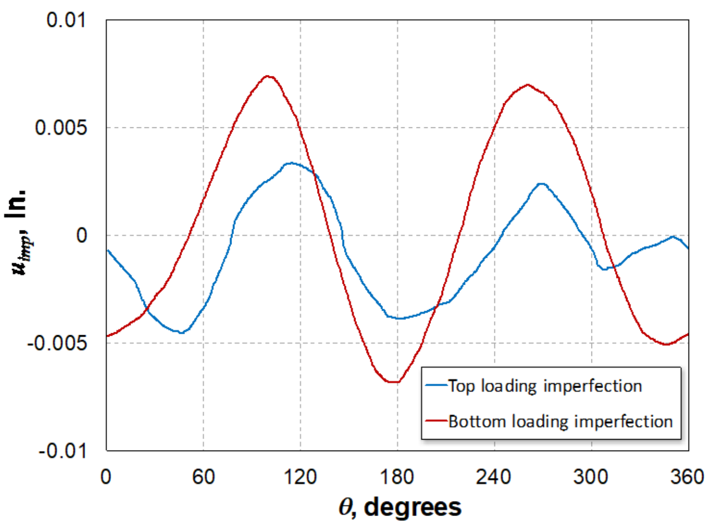

- Small effect on buckling load (-1.8%).
- Buckling initiate location moved from weld land A/B to weld land B/C, as observed in test

Highlighted Result (Metallic)

- **Metallic Buckling (continued)**

  M-3. Weld lands can reduce the buckling load of a compression-loaded cylinder.

  – **Addition of weld lands to integrally stiffened metallic cylinders led to a predicted reduction in linear buckling load between 1 and 27.6%.**

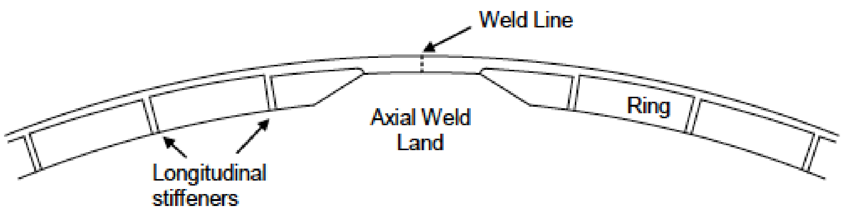

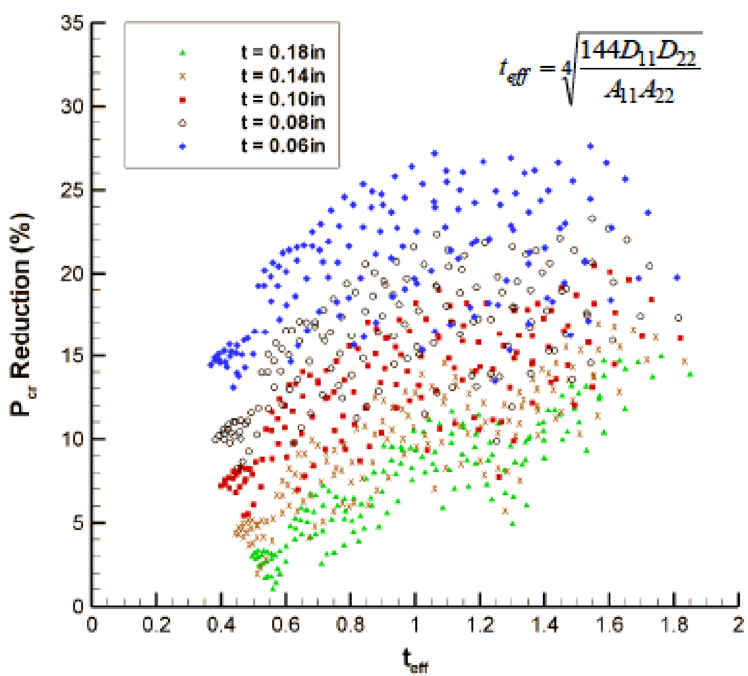

Buckling modes - Ares-I LH2

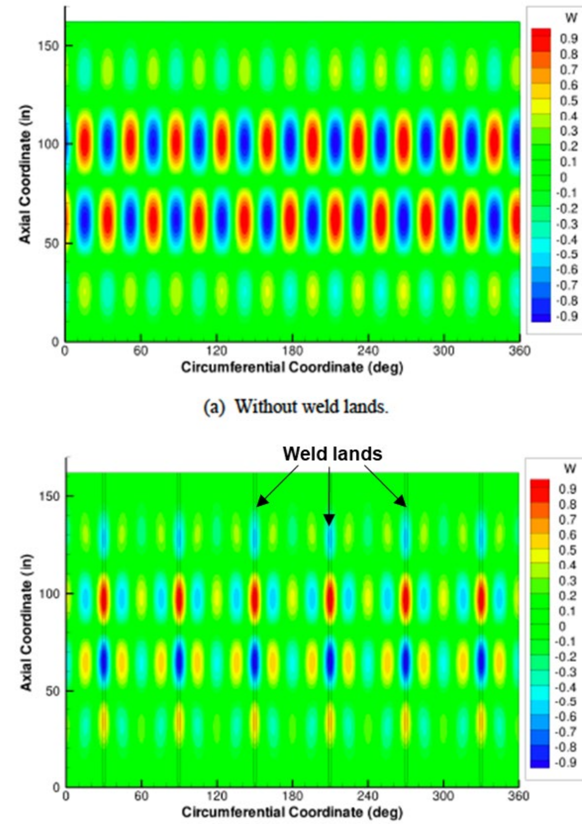

(a) Without weld lands.

(b) With axial weld lands.

Highlighted Result (Metallic)

- **Metallic Buckling (continued)**

M-4. Measured geometric imperfections of integrally stiffened cylinders with axial weld lands indicate relatively large magnitude localized imperfections at the weld lands.

8-ft-dia. cylinder with 3 weld lands

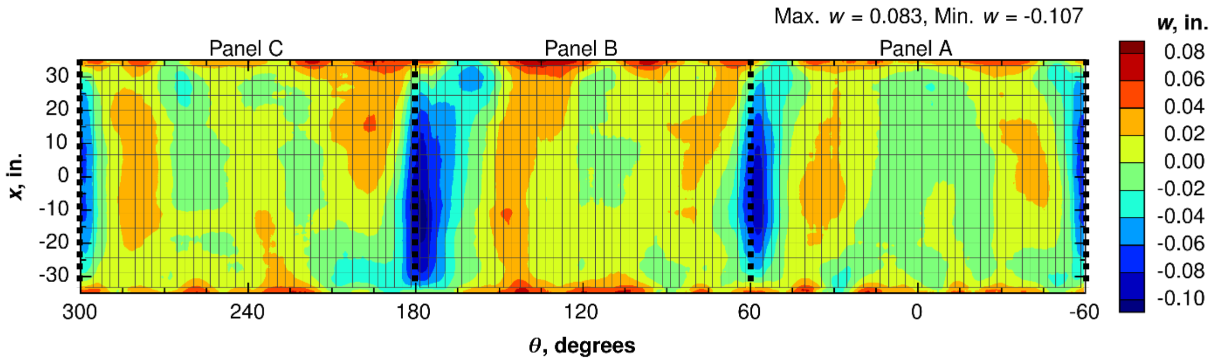

27.5-ft-dia. cylinder with 8 weld lands

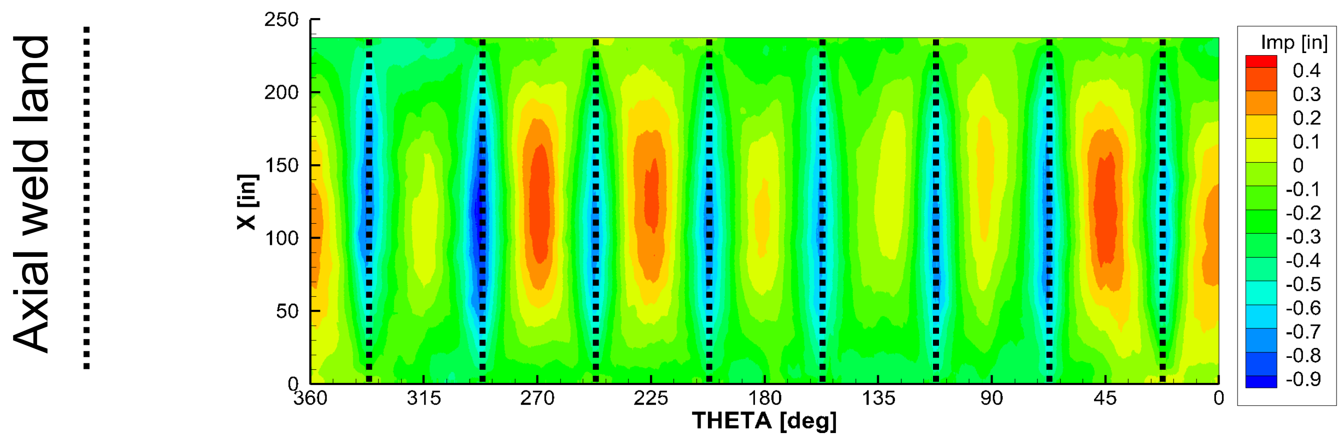

Highlighted Results (Composite)

C-1. The measured geometry of three of the 8-ft-diameter CTAs changed significantly between fabrication and the completion of the installation in the test facility, which resulted in changes to their structural response.

C-2. Geometrically nonlinear shell-element-based FEA were shown to provide accurate predictions of the buckling response (i.e., buckling load within 1.5%, 1%, and 7%) of the three large-scale buckling-critical sandwich CTAs tested.

C-3. To obtain the best quantitative and qualitative test-analysis agreement for the large-scale composite buckling tests (buckling load within 1.5%, 1%, and 7%) required the measured radial and thickness imperfections in the as-installed condition.

C-4. The use of multiple appropriate NDE techniques (e.g., thermography, shearography, ultrasound, visual inspection, geometry measurements, etc.) was necessary because each technique could used to detect potential defects or damage with different efficacy.

C-5. A multiscale speckle pattern where the local pattern was embedded within the larger global pattern was demonstrated on test articles CTA8.3 and CTA8.2B to be effective for obtaining high-resolution local DIC data over a subset of the lower-resolution global DIC area.

C-6. Damage detected using NDE on the large-scale composite test articles did not influence the global buckling behavior or failure.

Highlighted Result (Composite)

- **Composite Testing**

C-1. The measured geometry of three of the 8-ft-diameter composite test articles (CTAs) changed significantly between fabrication and the completion of the installation in the test facility, which resulted in changes to their structural response.

As-manufactured state (structured light scanning)

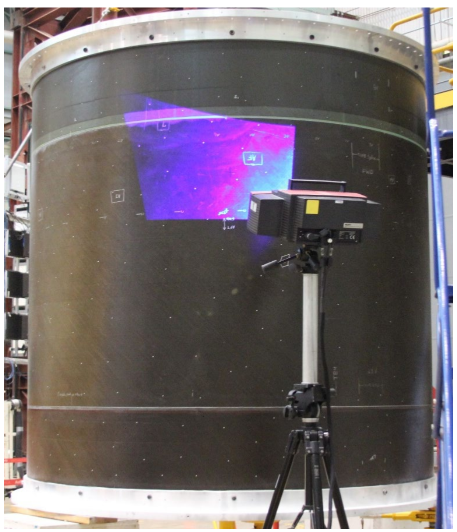

As-installed state (DIC)

Exterior surface radial position of CTA8.3

As-manufactured state

Radial position, in.

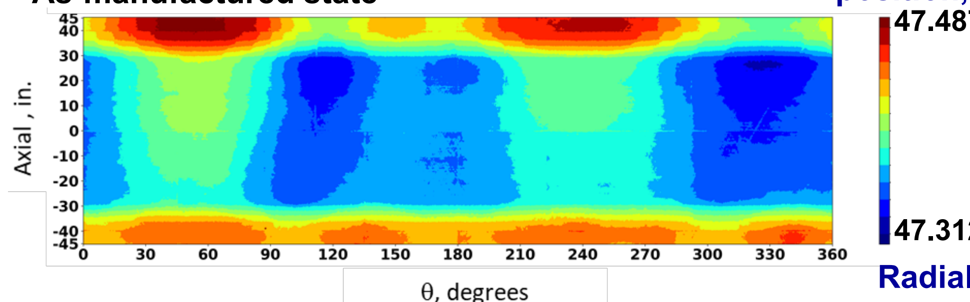

As-installed state at tare load

Radial position, in.

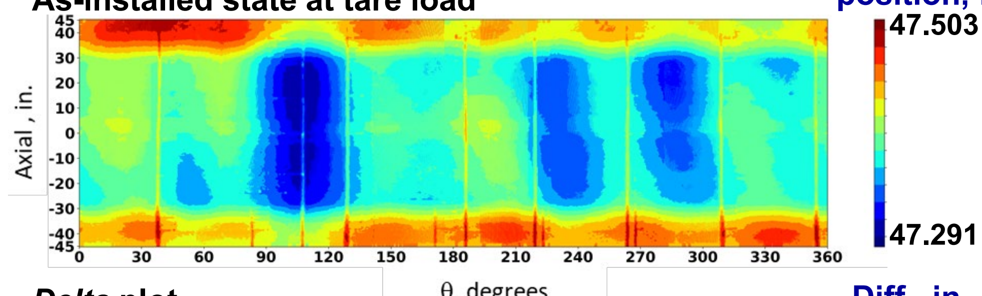

***Delta* plot**

Diff., in.

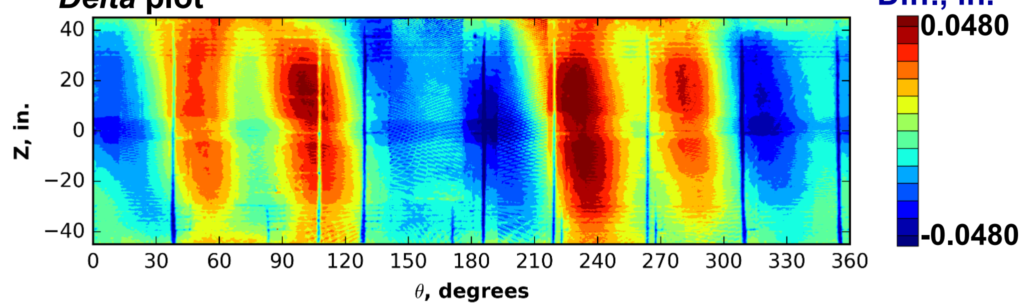

Highlighted Results (Composite)

- **Composite Buckling**

  C-2. Geometrically nonlinear shell-element-based FEA were shown to provide accurate predictions of the buckling response (i.e., buckling load within 1.5%, 1%, and 7%) of the three large-scale buckling-critical sandwich CTAs tested.

  C-3. To obtain the best quantitative and qualitative test-analysis agreement for the large-scale composite buckling tests (buckling load within 1.5%, 1%, and 7%) required the measured radial and thickness imperfections in the as-installed condition.

- **Finite element analysis**
  - Abaqus
  - Four-noded S4R shell elements
  - Layered-shell section definition
  - Implicit quasi-static transient analysis

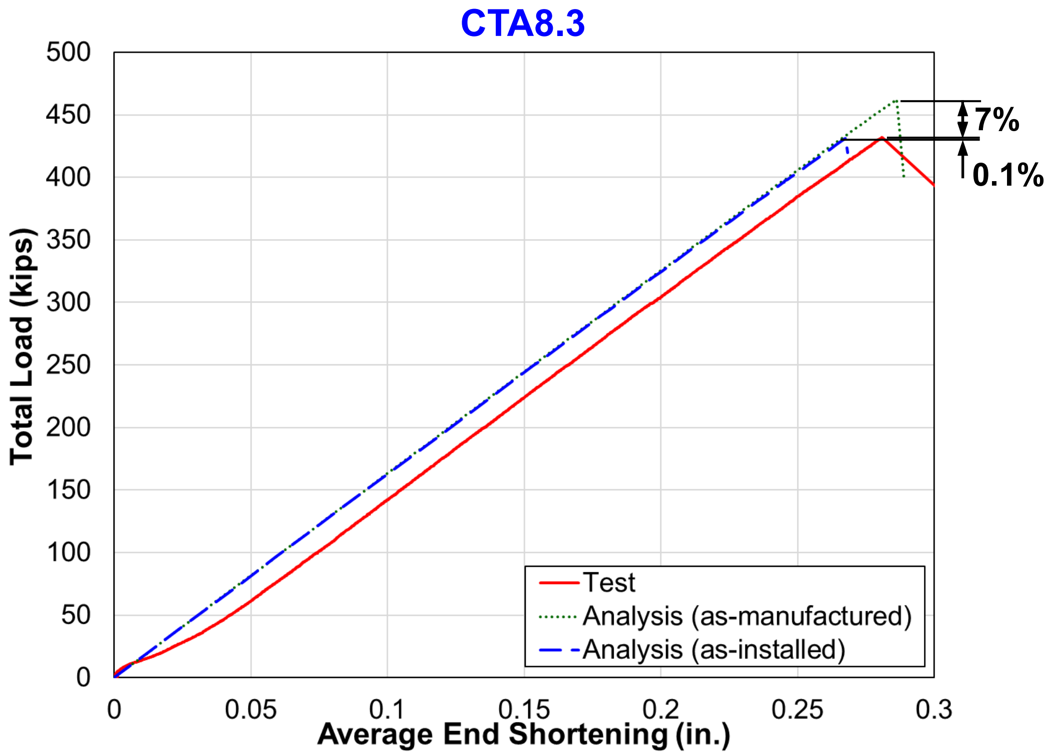

Highlighted Results (Composite) C-2 and C-3 concluded

- **Composite Buckling**

  C-2. Geometrically nonlinear shell-element-based FEA were shown to provide accurate predictions of the buckling response (i.e., buckling load within 1.5%, 1%, and 7%) of the three large-scale buckling-critical sandwich CTAs tested.

  C-3. To obtain the best quantitative and qualitative test-analysis agreement for the large-scale composite buckling tests (buckling load within 1.5%, 1%, and 7%) required the measured radial and thickness imperfections in the as-installed condition.

CTA8.2 radial displacement at 643 kips axial load

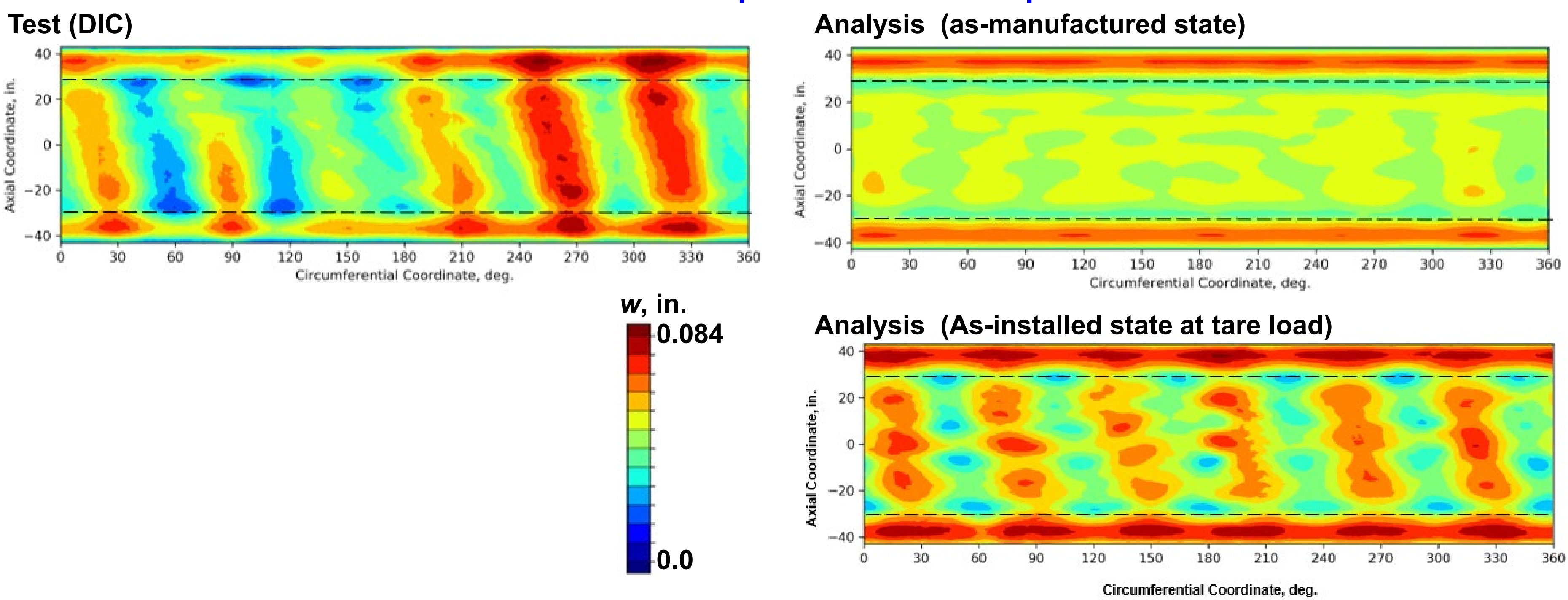

Highlighted Result (Composite)

- **Composite NDE**

  C-4. The use of multiple appropriate NDE techniques (e.g., thermography, shearography, ultrasound, visual inspection, geometry measurements, etc.) was necessary because each technique could used to detect potential defects or damage with different efficacy.

- **Test-article indications**
  - Visual inspection
    - Dry fiber
    - Fiber breakout
  - Thermography
    - Delaminations
    - Tow splices and overlaps
    - Film adhesive patch
  - Shearography (vacuum and thermal)
    - Core anomalies
    - Delaminations
    - Suggested low-velocity impacts
    - Core-to-facesheet disbonds
    - Padup disbond (secondary bond)
  - Geometry measurements
    - Nonvisible thickness changes related to damage

- **Ultrasound was difficult to apply to the thin-facesheet honeycomb core sandwich shells**

Thermal shearography

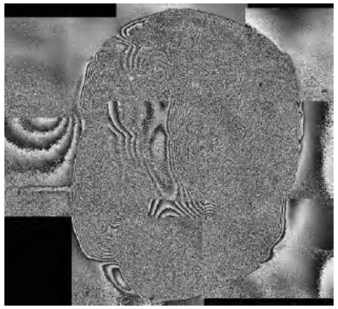

10x15 in. padup disbond (CTA8.1)

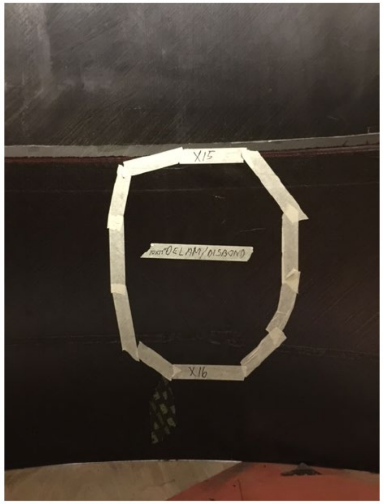

Highlighted Result (Composite)

- ## Composite Testing

  C-5. A multiscale speckle pattern where the local pattern was embedded within the larger global pattern was demonstrated on test articles CTA8.3 and CTA8.2B to be effective for obtaining high-resolution local digital image correlation (DIC) data over a subset of the lower-resolution global DIC area.

- **Global-local DIC**
  - NDE revealed several indications on CTA8.3 and CTA8.2B that were of some concern
  - Higher resolution DIC at these indications was desired to more closely monitor response
  - Technique adapted from Bomarito, Hochhalter, and Ruggles, *Experimental Mechanics*, 2018
  - Optimized multiscale pattern printed on temporary tattoo paper and applied to surface
  - Good correlation seen between global and local systems

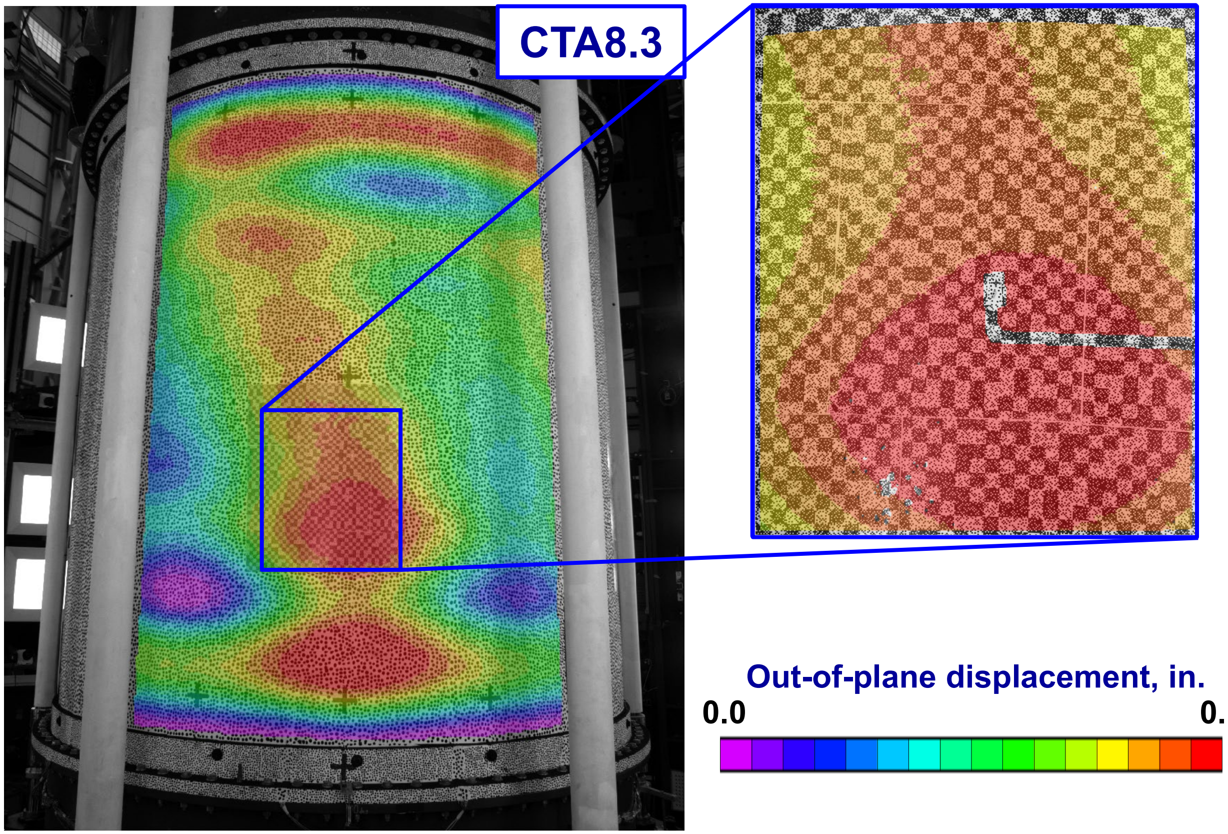

Highlighted Result (Composite)

- **Composite Testing**

  C-6. Damage detected using NDE on the large-scale composite test articles did not influence the global buckling behavior or failure.

- There were NDE indications on each of the composite test articles
  - CTA8.1 had many indications associated with the secondarily bonded padups
    - Many small disbonds on the forward padups
      - Repairs were unsuccessful
      - Test article was shortened to remove padup and new padup was applied
    - One large disbond on the aft inside padup
      - Disbonded region was removed and repaired with a scarf patch
    - Dry fiber found on inside surface
    - There were no indications that the identified/repaired damage influenced the structural response

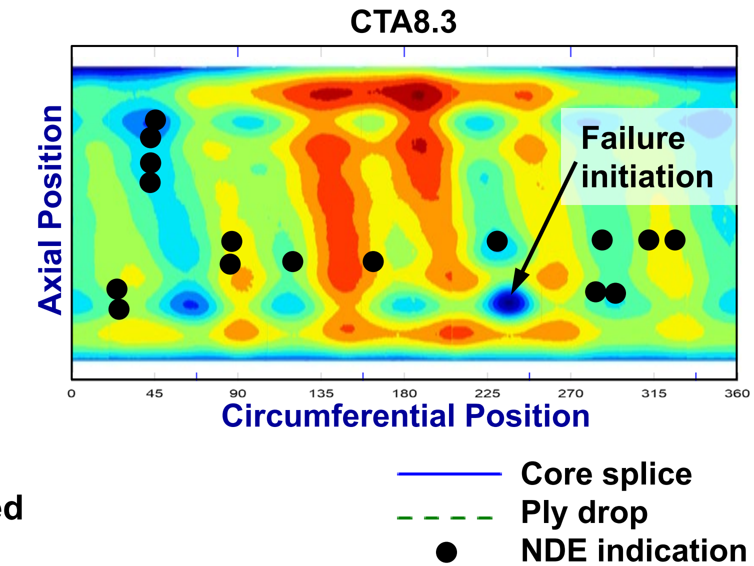

- Numerous small indications on CTA8.3, CTA8.2B
  - Primarily disbonds and core anomalies
  - Local DIC systems were set up on the indications that were potentially most detrimental
    - There was no indication (strain or displacement) that any of these damages influenced the stiffness-related behavior including buckling

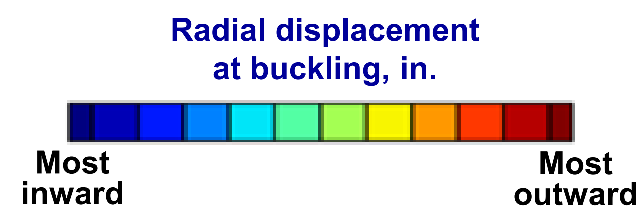

Concluding Remarks

- **Successful Assessment with many benefits to NASA and the Aerospace industry**
  - Multicenter team of experts
  - Workshops and collaborations with NASA, Industry, Academia, International partners
  - Led to a change in design practice
- **Revised the buckling design guidelines (SP-8007)**
  - State of the Art assessment that identifies important research developments and current trends and establishes the technological basis for the updated criteria and recommended practices.
  - New analysis-based KDF development approach and recommended practices

Concluding Remarks

- **Fifteen large-scale cylinder buckling tests completed**
  - Data used to develop and validate high-fidelity buckling predictions and analysis methods
  - These validated analysis methods are used to develop analysis-based KDF
- **Demonstrated benefits to SLS**
  - Mass and cost saving on Core Stage
  - Provide additional margin to support higher design loads
- **Information dissemination:**
  - ~60 SBKF publications (conference, journal, NASA report)
  - Numerous conference presentations and invited talks